Innovative Practice of Virtual Reality Technology in Animation Production

He Huixuan[1], Xiang Yuan[2]

Shijiazhuang University of Applied Technology, Animation Academy, Shijiazhuang City, Hebei Province, 050031, China

Abstract—In order to make the users who watch animation look better, the innovative practice research of virtual reality technology in animation production is proposed. According to the object structure information, the method uses 3ds Max software to complete the production of 3D animated character models. It completes the character prototype texture feature extraction through the character prototype boundary contour extraction, image hat height transformation, and discrete grid projection. The OpenGL texture mapping is used to complete the mapping of 3D animated character models. After the boundary optimization of texture seams, the best 3D animated character modeling effect is obtained. Geometric modeling technology and DOF nodes are used to build static and dynamic scene entity models to complete the construction of a 3D animation scene. The interactive visualization platform based on space is introduced to complete the visualization processing of the interactive animation scene, and the animation scene is regarded as the image base. The points with equal arc length are selected according to the curve points, and the camera is switched in combination with the roaming speed to realize the real-time roaming of 3D animation scenes and complete the innovative, practical application of virtual reality technology in animation production. Experimental results show that this method improves the smoothness, integrity, and authenticity of animation, improves the smoothness of motion, and ensures the real-time roaming effect.

Keywords—Virtual reality technology; animation production; 3D modeling; OpenGL; geometric modeling; real time roaming

I. INTRODUCTION

Virtual reality is a new world created by computer and electronic technology. It is a seemingly real simulation environment. Through a variety of sensor devices [1], [2], users can use people's natural skills to investigate and operate objects in the virtual world according to their feelings, participate in events in the virtual world, and provide intuitive and natural real-time perception of seeing, listening, and touching, and make participants "immerse" in the simulation environment [3]. 3D animation modeling technology is to create the structure and shape of objects involved in animation in the process of animation production. The modeling process requires the analysis of the shape characteristics of the object. The existing shape in the computer can be expanded and changed to meet the requirements of realistic modeling. In addition, the structure should also be linked with the geometry in reality. Through the analysis of object categories, different methods of model building and detail modification can be carried out [4].

Many researchers have conducted research on the application of virtual reality technology in animation production, such as Kokaram A et al. [5], who studied motion-based frame interpolation in film and television production. Frame interpolation is the process of synthesizing new frames between existing frames in image sequences. The difference frame is used as a key algorithm module in movie production to improve the effect of movie production. But motion-based frame interpolation usually requires a lot of computation and processing, especially in high-resolution image sequences. This may lead to excessive consumption of computing resources, reduce real-time performance, and increase production costs. For example, Khalid N et al. [6], to improve the accuracy of character modeling in the animation, through the Gaussian mixture model, each pixel of different human body parts is assigned a specific label to achieve better animation character modeling. However, this method has high requirements on the quality of input images. For low-quality, fuzzy or noisy images, the accuracy of joint extraction and pixel-level marking may decrease, thus affecting the accuracy of character modeling. Perez Perez Y et al. [7], to better complete the animation scene, proposed an environment modeling method based on joint semantic and geometric features, based on Markov random field (MRF), strengthen the consistency between environmental semantics (e. g., beam, column, wall, ceiling, floor, pipe), and geometric labels (example, horizontal, vertical, cylindrical), and use the neighborhood context to improve the accuracy of semantic labels, improve the accuracy of environment modeling, provide effective environment modeling basis for animation. However, when the environment is more complex or there are subtle changes, such as texture differences, lighting changes, etc., the method may encounter challenges in the consistency of semantic and geometric labels, resulting in a decline in the accuracy of modeling results.

Aiming at the problems existing in the above methods in 3D animation modeling, this paper combines virtual reality technology to study the innovative practice of virtual reality technology in animation production to provide users with a better 3D animation perception. The research structure of this article includes:

1) Provide a detailed introduction to the process and steps of using 3DsMax software to create character models, explain the methods of extracting texture features from character prototypes, including boundary contour extraction, image high-low hat transformation, and discrete mesh projection, and explain the application of OpenGL texture mapping technology and boundary optimization texture seam method;

2) Explain the application of geometric modeling technology and the construction process of DOF nodes, and

introduce the establishment of static and dynamic scene entity models;

3) Deeply explain the application of spatial based interactive visualization platforms and discuss the interactivity and visualization processing methods of animation scenes;

4) Introduce the concept and methods of treating animation scenes as image bases, and explain the application of techniques such as curve point filtering, camera switching, and roaming speed;

5) Verify the effectiveness of the techniques presented in this article through experiments;

6) Discuss the research results and point out future research directions.

II. ANIMATION PRODUCTION BASED ON VIRTUAL REALITY TECHNOLOGY

A. 3D Character Modeling

1) 3D animated character model based on 3ds Max*:* To build 3D models of related objects in animation, first, we need to analyze the structural characteristics of objects. The objects in 3D animation can be generally divided into two types: regular objects and irregular objects. There are two main modeling methods for animated 3D characters: the stacking modeling method and the subdivision modeling method. The stacking modeling method creates characters from details to the whole, while the subdivision modeling method first creates an object's overall shape and then carves details [8].

Regular objects are suitable for stacking modeling because of their regular shape. Its modeling process is to split complex objects into some basic components, then use the basic molding command to make these small parts and stack them together. Animation designers must grasp the model's size-scale relationship and spatial location. Common tools include insert, extrusion, turning, chamfering, FFD deformation tools, etc.

Irregular objects are more suitable for the subdivision modeling method; that is, the basic geometry is used to complete the large shape of the object first, and then the model details are subdivided by editing polygons or mesh editing tools. This modeling method is similar to drawing sketches or sculpture's construction process. Generally, we use subdivision modeling to complete the modeling of 3D characters, cartoon characters, or surface object bodies. Common tools include edit mesh, edit polygon, symmetry, mesh smoothing, etc. The specific process is shown in Fig. 1.

After determining the construction method, this paper completes the production of a 3D animated character model by applying the 3ds Max software, obtains the rough image by stretching and changing the graphics tools contained in the 3ds Max software, and then modifies the details with the modification tools, to establish a more accurate and intuitive model.

2) Character prototype texture extraction: The texture is an important feature of the scenery. It is generally believed that texture is a certain regularity of grayscale or color distribution on the image, which has different characteristics in complex textures. Texture can be roughly divided into two categories: regular and irregular. The extraction of irregular regional textures is an important part of image processing technology, so it has become a research hotspot of computer application technology.
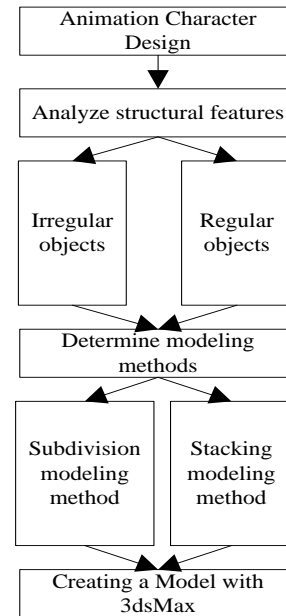

Fig. 1. Animation character modeling process.

a) Boundary contour extraction: The mathematical expression of the object contour obtained from the object image is called contour extraction [9], which is one of the basic steps in image processing, computer vision, and medical images.

This paper uses a method based on an improved model to extract the contour of the character prototype. Firstly, the method of combining some algorithms with the circumscribed rectangle is used to realize the automatic setting of the control points of the initial contour line of the model and then improve the gradient energy function to introduce the gradient vector flow operator so that the contour can better converge to the target depression, and adjust the weight of other energy function terms according to the actual situation. Finally, the target contour line is obtained through the neighborhood greedy algorithm when the total energy is minimized.

b) Image preprocessing: This paper combines high hat transform, and low hat transform to process the image. Add the high hat transform image to the original image, and then subtract the low hat transform image to get the enhanced image. Using the original image plus the result of the high hat transform can make the area with a larger gray value brighter, and subtracting the result of the low hat transform can make the smaller gray value darker. In this paper, the morphological reconstruction method is defined as:

$$C_{top}(f) = S_f(f) + 1 \qquad (1)$$

$$I = thresh\left(S_f(f)\right) \qquad (2)$$

Among them $S_f(f)$ is from the enhancement diagram at the start of the reconstruction operation, which is equivalent to subtracting a constant from the grayscale of the enhancement image $S_f(f) = f - h$, denoted by $S_f(f - h)$. Here is a marked graph. This paper binarizes the reconstructed result graph to get the marked graph. Because of the filtering effect of the reconstruction operation, many of the original images after the reconstruction operation are smaller than all the small peaks that will be "flattened". The value represents the size of the filtering amount [10]. In terms of filtering effect, reconstruction filtering is low-pass filtering, which flattens the peaks in the image. The peak in the image is the high-frequency part, and flattening the peak is equivalent to filtering out part of the high-frequency part. The low-frequency part is retained to form a low-pass effect.

The dual operation of reconstruction transformation is expressed as, according to the principle of dual operation, $S_f * (f + h)$ the role of will fill the low valley in the image. After operation $S_f * (f + h)$, it will be less than fill in the original low valley and form a platform at the original low valley. The combination of morphological and dual reconstruction can flatten the peak and fill the valley, leaving only the middle part of the image that is neither high nor low. The function of the parameter is to control the contrast. Generally, the contrast in the signal is less than all fluctuations that $2hh$ are filtered out.

Reconstruction filtering is essentially an efficient nonlinear filtering, and the filtering effect is similar to median filtering, but the effect is better. The purpose of morphological reconstruction is to extract the maximum value and bright top of the region to smooth the interior of each target and extract the maximum value within the target range.

c) Texture extraction: Generally, texture images are stored and represented rectangularly [11]. This exactly corresponds to the discrete grid of the surface, which is the points on the discrete grid are projected onto the image, and the color information of the image is extracted so that the texture is arranged in the form of a discrete grid, but this is too sparse. Therefore, the mesh needs to be refined. Each refined mesh point corresponds to a pixel on the texture image. Original geometric mesh size is 4×3, to extract texture, each geometric mesh is further uniformly refined 4×4. The size of the whole refined mesh is 16×12. Each vertex on the mesh corresponds to a pixel of each vertex that is re-projected onto the image (in the actual solution process, both the vertical grid line and the horizontal grid line corresponding to the grid point can be projected onto the image to find the intersection point on the image). The color information of the point on the image is obtained to form a texture image [12]. The coordinate value of the thinned image point is usually a floating point number. If the color value of one of its neighboring pixels is directly taken as the color value of the current point, the extracted texture will become more blurred.

Therefore, in this paper, color information is extracted in a weighted way according to the position of the current point and the proximity of the four adjacent pixels around it, as shown in Fig. 2, (x, y) is the pixel coordinate of the current image point,

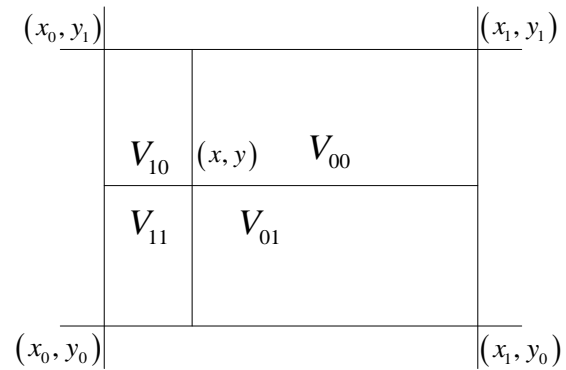(x_1, y_0) is the coordinate of four adjacent pixels (the coordinate value is an integer).

Fig. 2. Weighted center of gravity.

Set $f(x, y)$ is a point the texture extraction based on barycentric coordinates can be expressed as:

$$f(x, y) = \frac{c_{top}(f)}{I} \frac{V_{00}}{V} f(x_0, y_0) + \frac{V_{01}}{V} f(x_0, y_1) \qquad (3)$$
$$+ \frac{V_{10}}{V} f(x_1, y_0) + \frac{V_{11}}{V} f(x_1, y_1)$$

The whole surface is projected onto the front view, and the barycentric weighted texture extraction method can be used to obtain the image's texture. For the texture data matrix [13] outside the specified area, please give it a uniform value of 0 and give the part of the texture data matrix outside the texture outline in the specified area a value of 1. This aims to facilitate the storage of irregular regional textures and the subsequent mapping of 3D models.

3) Model mapping and optimization

a) Model mapping based on OpenGL texture mapping: After getting the texture image and 3D model, we need to use its projection relationship to give the corresponding texture information to the corresponding part of the image on the surface of the 3D model, that is, local texture mapping. Texture mapping technology is also called texture mapping technology [14]. In 3D graphics, texture mapping methods are widely used, especially to describe realistic objects. The work of local texture mapping is to correctly back project an acquired texture image onto the surface of the 3D model.

This paper uses OpenGL texture mapping technology to map 3D models. The technology of texture mapping of the texture image refers to mapping the texture image to the surface of a three-dimensional object, that is, predefine the texture pattern on the texture space of a plane area and then establish the mapping relationship between the object surface space and the coordinates of the texture pattern. When the visible points of the object's surface are determined, the texture pattern can be attached to the object's surface according to the value of the corresponding points in the texture space. The general steps of texture mapping are shown in Fig. 3.

Start

Define Texture Graphics

Control Texture

Specify texture mapping method

Define texture coordinates

Determine the three-dimensional coordinates of the drawing

Establish mapping relationships for graphic mapping
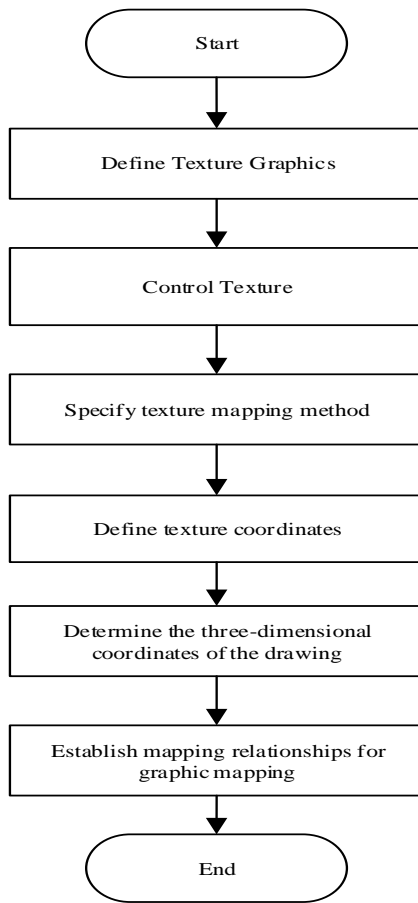
End

Fig. 3. Texture mapping steps.

For relatively flat model areas, texture mapping is relatively easy to implement. This paper introduces merging adjacent triangular patches to deal with irregular mapping areas. Its algorithm idea takes the included angle between the normal vectors of adjacent triangular patches as the object of study. The included angle will remain unchanged if it exceeds a set closed value. If the included angle is less than a certain idle value, it will merge two triangular patches, and so on repeatedly. However, since the included angles of multiple triangular patches may accumulate in the same direction during the merging process, if it is possible to simplify the larger surface into a plane according to the above principles, limiting the size of the composite surface is necessary. When the area of the plane is greater than a set value, the merging stops. According to the corresponding texture area of the model surface, the merged plane can use the trilinear filtering texture filtering technology to operate it in OpenGL to achieve relatively flat texture mapping of the model area. To map the bump model surface, it is necessary to comprehensively consider the texture's stretching, scaling, bending, and the change of gray value. See Fig. 4 for details.

As shown in Fig. 4, a texture segment $O*P*$ is for the curve segment of the bump model; the texture segments attach to the curve segment $O*P*$, assume that in the curve segment: $O*Q*=w, Q*R*=v, R*P*=u$.
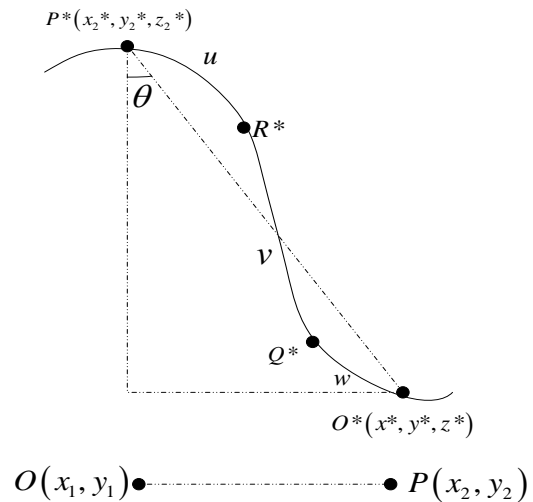

Fig. 4. Schematic diagram of concave-convex texture processing.

To stretch a texture segment OP, which also means reducing the length of the distance between and $P*$. Make line segment OP and $O*$ and $P*$ the included angle between is θ, then represent:

$$\sin\theta = \frac{|OP|}{|O*P*|} = \frac{f(x,y)\sqrt{(x_1-x_2)^2(y_1-y_2)^2}}{\sqrt{(x_1*-x_2*)^2(y_1*-y_2*)^2(z_1*-z_2*)^2}} \tag{4}$$

To make the length of texture deformation the same as the curve, the interpolation coefficient is introduced here. Setting rules are as follows:

When a surface moves from a point to point $Q*$, take $s = o$;

When a surface moves from a point to point $R*$, take $s = q$;

When a surface moves from a point to point $P*$, take $s = r$;

And:

$$ow + qv + ur = |OP| \tag{5}$$

$$o + q + r = 1 \tag{6}$$

Can get

$$\sin\theta = \frac{|OP|}{|O*P*|} = \frac{ow+qv+ur}{\sqrt{(x_1*-x_2*)^2(y_1*-y_2*)^2(z_1*-z_2*)^2}} \tag{7}$$

After the above transformation, the texture space coordinates can be mapping area coordinates with the bump model one-to-one correspondence to better realize bump model mapping.

b) Boundary optimization*:* Because of the color difference of the texture at the back boundary of the texture mapping of the 3D character model, it is easy to have color discontinuity between the texture regions; that is, texture seams when rendering realistically. If not properly handled, it will greatly impact the reality of the 3D modeling of the character. Therefore, the purpose of processing texture boundaries is to eliminate texture seams in the display effect as far as possible.

The parameterization method is used to map the mesh model to the plane domain or other domains to process the model with some mature technologies in the parameter domain [15]. Parameterization is to establish a one-to-one correspondence between the vertices of the mesh model and the points on the parameter domain and ensure that the mesh formed by the vertices on the parameter domain is not folded. The deformation of the parameterized mesh is smaller than that of the original mesh. According to the different parameter domains, parameterization can be plane and spherical.

Planar parameterization is to spread the mesh model into a planar mesh. Each triangle uniquely corresponds to a triangle in the planar domain, which is helpful for texture mapping of the mesh. Spherical parameterization can map the completely closed mesh to the spherical domain, which is conducive to mesh simplification, shape gradient, and other processing.

According to the idea of parameterization, the implementation steps of texture seam processing at the back boundary of 3D character model texture mapping can be established: locate the triangle mesh belt on both sides of each boundary. The grid belt is parameterized in two dimensions; In parameter domain, texture is constructed by weighted interpolation method to achieve natural transition [16]. So far, this paper has completed the optimization of texture mapping.

B. 3D Animation Scene Construction based on Virtual Reality

The 3D solid model in a virtual scene generally includes static and dynamic solid modeling. Static refers to solid models of terrain and ground objects, ranging from houses, pavilions, and launchers to roadside flowers and trees. Dynamic solid models refer to various simulation solid models with motion attributes, such as pedestrians, robots, swing booms, etc.

1) Construction of scene static entity: The physical building is the main part of the virtual scene and the most important scene content. The modeling of static entities mainly uses geometric modeling technology [17]. Geometric modeling studies basic problems such as graphic data structure and deals with the representation of polygons, triangles, and points of objects' geometry and morphology, as well as their appearance, textures, materials, and colors. In the geometric modeling of solid buildings, it is required that the real and accurate space position and surface texture be used to represent the objective object of buildings to create an environment in which the observer can feel immersive and immersive. Geometric modeling is mainly realized by corresponding modeling software such as 3DMAX, AutoCAD, etc. 3D modeling of buildings is carried out in combination with AutoCAD and 3DMax [18]. The overall process includes total station acquisition of characteristic data points, importing AutoCAD and AutoLISP software to form wireframes, importing 3DMax to establish 3D models, 3DMax texture mapping, and model output. The overall process is shown in Fig. 5.
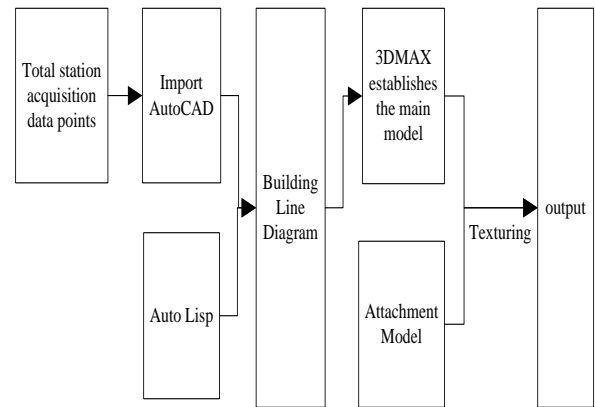
Fig. 5. Building 3D modeling based on AutoCAD and 3DMax.

2) Construction of dynamic entities: The modeling of moving parts should first construct moving objects. The construction of moving objects may change the initially built internal organization [19], that is, add DOF nodes of moving parts in the file formed by modeling, set corresponding local coordinates and locate them, and carry out the kinematic relationship (Link analysis) on multiple moving parts based on DOF to determine the kinematic traction relationship, determine and publish the main parts. The process of non-publicly distributed sub-components and traction equation is shown in Fig. 6.
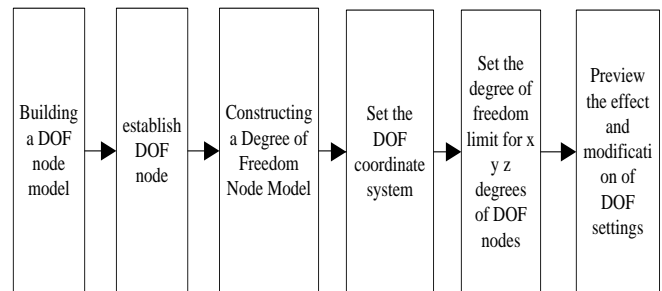
Fig. 6. General process of establishing DOF nodes.

C. Interactive Animation Scene Visualization

Animation design aims to establish a spatially based interactive visualization platform [20], integrating relational databases, spatial location files, component modules, various multi-dimensional graphical visualization tools, and common graphical expression tools. The above module takes relational data as the analysis object, applies spatial spatial analysis principles and methods to extract spatial information, and displays it as layers. The object is further analyzed and transformed through graphical visualization methods, such as a parallel coordinate method, to explore the inherent abstract rules of spatial data. These abstract rules are just beyond the reach of traditional spatial analysis and expert experience. Finally, appropriate visualization technology is selected to express the rules so that the rules or patterns contained in the data can be transformed into graphics that are easy to understand and recognize and visualized through animation. Fig. 7 is the visualization structure diagram of an interactive animation scene.
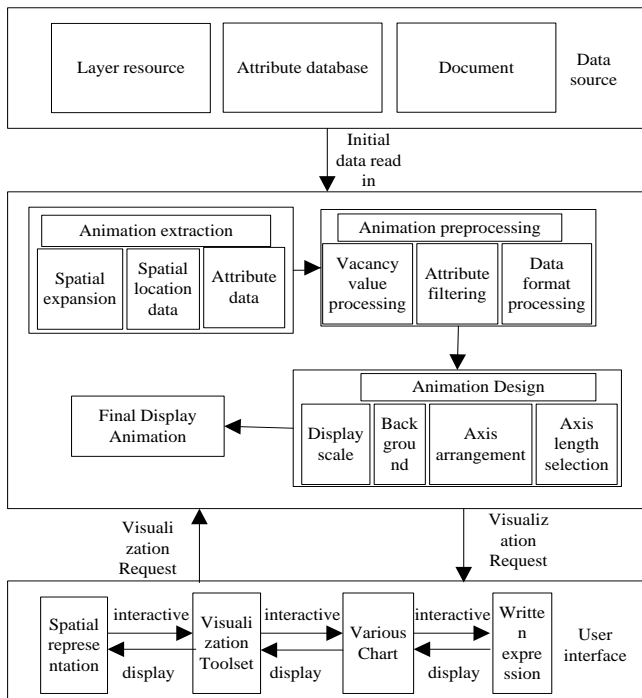
Fig. 7. Interactive animation scene visualization structure diagram.

As shown in Fig. 8, the main function of the space module is to provide a layer-calling function and a simple layer-editing function, such as refreshing, mouse response, highlighting, etc.; The main function of the visualization toolset module is to focus on implementing HyperTree and parallel coordinate method and provide a toolset management function to add or delete tools dynamically; The main function of the interaction function module is to realize the interaction between visualization tools and spatial layers, as well as between visualization tools.
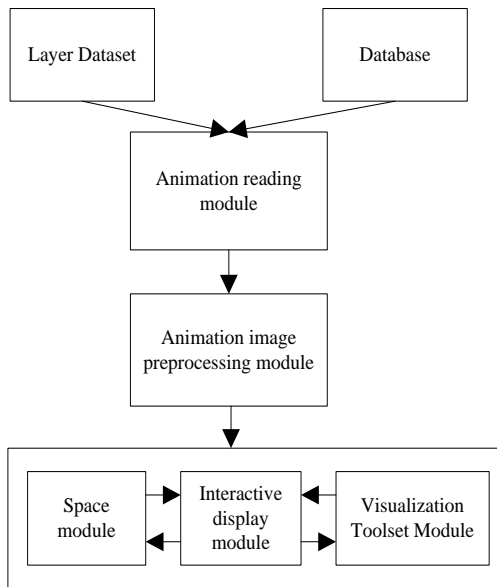

Fig. 8. Functional module structure diagram.

Layers and various multidimensional visualization tools each play an important role in interactive animation scene visualization. Layers display animation data and express spatial attributes of spatial objects. Graphic visualization tools are suitable for expressing nonspatial multidimensional attributes. Interactive animation scene visualization focuses on combining layers and multidimensional visualization tools [21] to develop their interactive functions. The interactive function in interactive animation scene visualization is shown in the following points:

1) HyperTree is used to manage hierarchical layer resources;

2) HyperTree highlighted nodes interact with corresponding layers [22];

3) The highlighted area on the layer interacts with the parallel coordinate, which displays the nonspatial attribute data of the area;

4) HyperTree highlights nodes to interact with parallel coordinates, which express the attribute information of corresponding layers;

5) The parallel coordinate method is used to compare and analyze the attribute data of each region on each layer [23].

To summarize, the layer you see, the highlighted node in the center of HyperTree, and the parallel coordinate visualization tool are all aimed at the same animation target object. After realizing interactive expression among layers, HyperTree expression, parallel coordinate expression, and common charts, the user's thinking is more coherent, and various tools give full play to their due advantages, showing a more advantageous interactive animation scene visualization effect.

D. Real-time Roaming of 3D Animation Scene

In the process of real-time roaming of the animation scene, first select three animation scenes in the three-dimensional space to form an image base, calculate the image overlap area, fuse the area, use this as the basis for image stitching [24], extract the color information of the animation scene image, calculate the sampled image data [25], obtain the curve points of the scene image, and filter points with equal arc length according to the curve points, Switch the camera according to the points with equal arc length and the roaming speed to complete the real-time roaming of 3D animation scene. The specific steps are detailed as follows:

Assumed represents 3D global coordinates, (x'_1, x'_2) represents two-dimensional plane coordinates, e represent the time variable, then use equation (8) to select three animation scenes in three-dimensional space to form an image base, calculate the overlapping area between images, and use equation (8) to express

$$\partial * (\mu) = \frac{[X'_1, X'_2, X'_3] \otimes (x'_1, x'_2)}{\sin \theta e \sigma[\gamma]} \tag{8}$$

Where $\sigma[\gamma]$ represents an image sequence.

Assumed represents the position of a point in the scene from the viewpoint, a represents the distance between the agreed viewpoint and the object, represents the brightness

difference of two adjacent images, then use Formula (9) to fuse the regions and sew the images according to this:

$$\overline{m}(G) = \frac{A(\wp) \times \eta}{a \times \partial} - \partial * (\mu)\mu(\alpha) \otimes [\Gamma(\theta)] \quad (9)$$

Where ∂ represents the tensor parameter, the camera position, and any point in the viewpoint grid.

Hypothesi n represents any time of roaming $\overline{m}(T)$ represents a viewpoint, the coordinates of this point determine a point on the image taken by the lens, and the color of this point is defined as the pixel color corresponding to the point expressed by Formula (10):

$$m * (\delta) = \frac{\overline{m}(T) \times n \overline{m}(G)}{\partial(\Upsilon)} \quad (10)$$

Where $\partial(\Upsilon)$ represents the pixel values of different image regions, $t(b)$ represents the color value between unit squares.

Assume the edge represents boundary conditions, Represents the tangent value of the curve, calculate the sampled image data using Equation (11), obtain the curve points of the scene image, and filter points with equal arc length according to the curve points:

$$g(c) = \frac{\theta(l) \times \Gamma m * (\delta)}{L(\sigma)} \times \varphi(\gamma) * \Phi(\mu) \quad (11)$$

Where $L(\sigma)$ represents the camera storage format, the arc length curve point set, and the jitter state in the walkthrough.

Assumed that represents the rotation angle of image coordinates, $\delta(j)$ represent the density value of curve points, use formula (12) to switch cameras according to points with equal arc length and roaming speed to complete real-time roaming of 3D animation scene:

$$\eta(\overline{m}) = g(c) \frac{\delta(j) * M(K)}{C(\mu)} \times \xi(\vartheta) \quad (12)$$

Where $\xi(\vartheta)$ represents roaming parameters, $C(\mu)$ represents the cumulative distance between points.

The above method is the principle of real-time roaming of 3D animation scenes, which is used to complete real-time roaming of 3D animation scenes [26].

III. EXPERIMENTAL ANALYSIS

To verify the innovative practice effect of this method in animation production, take the Judy police officer role and animation scene in the "Crazy Animal City" animation as an example; use this method to model, texture map, and virtual roaming interaction, and give the Judy police officer and scene produced by this method, as shown in Fig. 9.

(a) Character modeling

(b) Scene modeling

Fig. 9. Effect of the method mapping in this article.

It can be seen from the analysis of Fig. 9 that this method uses OpenGL texture mapping technology for mapping, which improves the effect of 3D animation design of characters and scene modeling, making both clearer and more realistic.

The method in this paper is used to conduct real-time roaming experiments on some scenes and characters in Crazy Animals to verify the practicability of animation scene construction, and the effect is shown in Fig. 10.

(a) 15 frames

(b) 25 frames

(c) 35 frames

(d) 45 frames

Fig. 10. Real-time roaming rendering.

As can be seen from Fig. 10, this paper selects three animation scenes in the three-dimensional space to form an image base. It combines the roaming speed to switch the camera and the points with the middle arc length of the image curve points to achieve real-time roaming to ensure the practical effect of real-time roaming.

The texture mapping of the character model is optimized by optimizing the boundary processing method in this paper to eliminate the texture seams in the display effect. The effect before and after optimization is shown in Fig. 11.

(a) Pre optimization rendering

(b) Optimized rendering

Fig. 11. Effect before and after optimization.

By analyzing Fig. 11, it can be seen that the boundary optimization method in this paper has a good effect on eliminating texture seams. It is clearer for the expression of the appearance and texture of animated characters, enhances the texture of animated characters, and verifies that the texture mapping map in this paper is more practical, making the animation effect smoother and giving users a better impression.

To verify the collision detection performance of the method in this paper, the experiment conducted collision detection on a virtual scene, and the results are shown in Fig. 12.

It can be seen from Fig. 12 that collision detection for real-time roaming in the virtual scene is carried out by the method in this paper. The detection time is only 4ms, and the detection time is less than 10ms. It can be seen that this method has good performance in collision detection of virtual scenes.
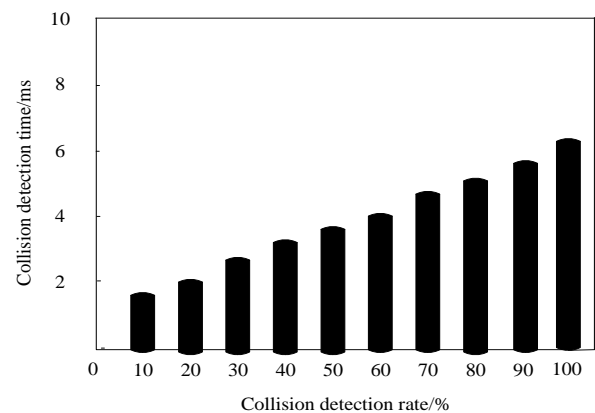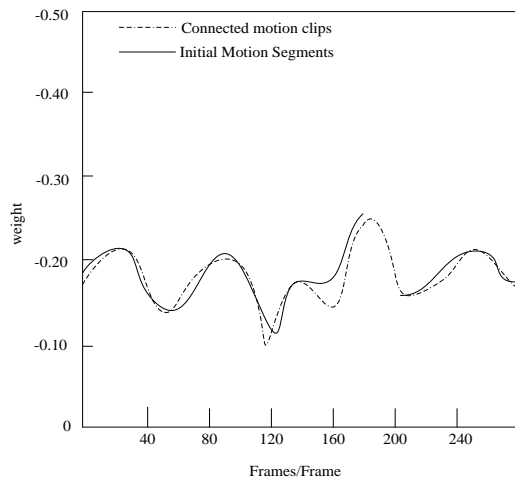

Fig. 12. Collision detection time and collision detection rate.

To verify the smoothness of the motion connection of the 3D animated character model in this method, the motion process of Police Officer Judy was tested. There are 30 frames in each motion clip, and the number of clips is 8, totaling 240 frames. The connection smoothness in the ear joint and eye rotation motion segment of police officer Judy in the post-application test of this method is shown in Fig. 13.

(a) The Movement Process of Ear Cartilage Joints
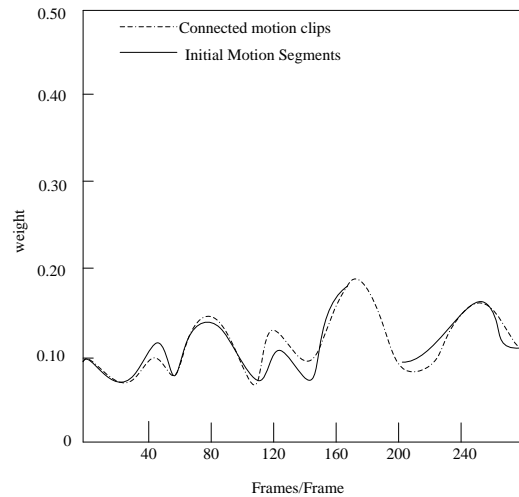
(b) The movement process of eye rotation

Fig. 13. Connection smoothness of two motion segments.

From the analysis of Fig. 13, it can be seen that through the method in this paper, the connection between the two motion segments is relatively smooth, and the initial motion is also retained accordingly. The experimental results show that the connection smoothness of each part of the motion segment is high under the method in this paper. Applying this method to animation production can enhance the visual perception of animation and bring a good visual experience.

IV. CONCLUSION

Aiming at the problems of low fluency and rough models in 3D modeling animation production, the innovative practice of virtual reality technology in animation production is studied to improve the animation user perception. Animated character modeling, image texture extraction, mapping, and optimization are realized through 3ds Max software. The animation scene is constructed from the two entry points of dynamic entity and static entity, and through interactive animation scene visualization design and 3D animation scene real-time roaming design, the innovative practice of virtual reality technology in animation production is finally realized. Through experimental verification, this method can improve the quality of animation production and enhance the visual perception of users. In addition, in future animation production, researchers can work to introduce more complex and realistic physical effects, such as cloth simulation and liquid simulation, to provide more realistic visual effects for animation production, and enhance the user's immersion and viewing experience.

COMPETING OF INTERESTS

The authors declare no competing of interests.

Authorship Contribution Statement. Xiang Yuan: Writing-Original draft preparation, Conceptualization, Supervision, Project administration.

He Huixuan: Language review, Methodology, Software

DATA AVAILABILITY

On Request

DECLARATIONS

Not applicable

REFERENCES

[1] D. A. Purwaningsih, "Puppet movements in structure-specific traditional paper cut out animation production," Ultimart: Jurnal Komunikasi Visual, vol. 13, no. 2, pp. 61–68, 2020.

[2] F.-L. Wu, H. Liang, C. Ge, F. Liang, Q. Zhang, and J.-Z. Lu, "Semantic Framework Promotes Interactive Puppetry Animation Production to Assist Storytelling Training.," Journal of Information Science & Engineering, vol. 36, no. 6, 2020.

[3] M. Akdere, K. Acheson, and Y. Jiang, "An examination of the effectiveness of virtual reality technology for intercultural competence development," International Journal of Intercultural Relations, vol. 82, pp. 109–120, 2021.

[4] L. Zhang, M. Boutaous, and S. H. Xin, "3D Modeling of Polymer Selective Laser Sintering Process: Laser-Polymer Interaction Modeling," Key Eng Mater, vol. 926, pp. 349–357, 2022.

[5] A. Kokaram, D. Singh, S. Robinson, D. Kelly, B. Collis, and K. Libreri, "Motion‐based frame interpolation for film and television effects," IET Computer Vision, vol. 14, no. 6, pp. 323‐338, 2020.

[6] N. Khalid, Y. Y. Ghadi, M. Gochoo, A. Jalal, and K. Kim, "Semantic recognition of human-object interactions via Gaussian-based elliptical modeling and pixel-level labeling," IEEE Access, vol. 9, pp. 111249–111266, 2021.

[7] Y. Perez-Perez, M. Golparvar-Fard, and K. El-Rayes, "Segmentation of point clouds via joint semantic and geometric features for 3D modeling of the built environment," Autom Constr, vol. 125, p. 103584, 2021.

[8] A. M. Pessoa, I. M. Guerreiro, C. F. M. e Silva, and F. R. P. Cavalcanti, "A Positive Semidefinite Autocorrelation Function for Modeling 3D Gaussian processes," IEEE Trans Veh Technol, vol. 70, no. 2, pp. 1941–1945, 2021.

[9] R.-W. Bello, A. S. A. Mohamed, and A. Z. Talib, "Contour extraction of individual cattle from an image using enhanced Mask R-CNN instance segmentation method," Ieee Access, vol. 9, pp. 56984–57000, 2021.

[10] A. Bajaj, R. Khurana, and M. E. Ali, "Quantum Interference and Spin Filtering Effects in Photo-responsive Endoperoxide Based Single Molecular Device," 2021.

[11] M. Khojastehnazhand and M. Roostaei, "Classification of seven Iranian wheat varieties using texture features," Expert Syst Appl, vol. 199, p. 117014, 2022.

[12] G. Guingo, F. Larue, B. Sauvage, N. Lutz, J.-M. Dischler, and M.-P. Cani, "Content-aware texture deformation with dynamic control," Comput Graph, vol. 91, pp. 95–107, 2020.

[13] J. Yang, S. Zhong, V. Luzin, J. Li, X. Liu, and C. Dan, "HRTex: a high-resolution texture data processing tool for monochromatic neutron diffraction based on the pixel projection method," J Appl Crystallogr, vol. 55, no. 2, pp. 425–435, 2022.

[14] K. Chaiyasarn, A. Buatik, H. Mohamad, M. Zhou, S. Kongsilp, and N. Poovarodom, "Integrated pixel-level CNN-FCN crack detection via photogrammetric 3D texture mapping of concrete structures," Autom Constr, vol. 140, p. 104388, 2022.

[15] L. Dumitru, "Evolution of force‐free field parameter in active regions with major eruptive events," Astronomische Nachrichten, vol. 342, no. 3, pp. 485–496, 2021.

[16] Z. Ni, Y. Liu, J. Xie, Y. Liao, and J. Dai, "Investigation on the Design Method and Failure Mechanism of Silicon-Based MEMS Setback Arming Device," in International Conference on Mechanical Design, Springer, 2021, pp. 2357–2374.

[17] H. Liu, S. Xu, and S. Liu, "An online course mode based on microlecture videos: Using CAD geometric modeling course as an example," Computer Applications in Engineering Education, vol. 29, no. 5, pp. 1300–1311, 2021.

[18] W. Xu, P. Liu, and Z. Lu, "Research on digital modeling and optimization of virtual reality scene," International Journal of Advanced Network, Monitoring and Controls, vol. 3, no. 4, pp. 69–76, 2019.

[19] S. Zhu, G. Yu, W. Tang, J. Hu, and E. Luo, "Thermoacoustically driven liquid-metal-based triboelectric nanogenerator: A thermal power generator without solid moving parts," Appl Phys Lett, vol. 118, no. 11, 2021.

[20] K. Zhao et al., "Interactively mechanochromic electronic textile sensor with rapid and durable electrical/optical response for visualized stretchable electronics," Chemical Engineering Journal, vol. 426, p. 130870, 2021.

[21] H. Dou, B. Xu, F. Shen, and J. Zhao, "V-SOINN: A topology preserving visualization method for multidimensional data," Neurocomputing, vol. 449, pp. 280–289, 2021.

[22] G. Gottlob, M. Lanzinger, R. Pichler, and I. Razgon, "Complexity analysis of generalized and fractional hypertree decompositions," Journal of the ACM (JACM), vol. 68, no. 5, pp. 1–50, 2021.

[23] S. Zou, H. Liu, Y. Liu, J. Yao, and H. Wu, "Singularity Analysis and Representation of 6DOF Parallel Robot Using Natural Coordinates," Journal of Robotics, vol. 2021, pp. 1–11, 2021.

[24] L. Nie, C. Lin, K. Liao, and Y. Zhao, "Learning edge-preserved image stitching from multi-scale deep homography," Neurocomputing, vol. 491, pp. 533–543, 2022.

[25] X. Zhou et al., "Extracting photometric redshift from galaxy flux and image data using neural networks in the CSST survey," Mon Not R Astron Soc, vol. 512, no. 3, pp. 4593–4603, 2022.

[26] A. Rosinol et al., "Kimera: From SLAM to spatial perception with 3D dynamic scene graphs," Int J Rob Res, vol. 40, no. 12–14, pp. 1510–1546, 2021.